Mechanism of the Two-electron Reduction of *trans*-Oxoaquaruthenium(IV) to *trans*-Diaquaruthenium(II) †

Chi-Keung Li, Chi-Ming Che,* Wai-Fong Tong and Ting-Fong Lai
Department of Chemistry, University of Hong Kong, Pokfulam Road, Hong Kong

The kinetics and mechanism of the reduction of *trans*-$[Ru^{IV}L(O)(H_2O)]^{2+}$ to *trans*-$(Ru^{III}L(OH)(H_2O)]^{2+}$ (L = 6,7,8,9,10,11,17,18-octahydro-6,10-dimethyl-5*H*-dibenzo[*e*,*n*][1,4,8,12]dioxadiazacyclopentadecine) in aqueous solution by *cis*-$[Ru^{II}(NH_3)_4(isn)_2]^{2+}$ (isn = isonicotinamide) and of *trans*-$[Ru^{III}L(OH)(H_2O)]^{2+}$ to *trans*-$[Ru^{II}L(H_2O)_2]^{2+}$ by $[Ru^{II}(NH_3)_4(bipy)]^{2+}$ (bipy = 2,2′-bipyridine) have been studied. The reactive intermediates are *trans*-$[Ru^{IV}L(OH)(H_2O)]^{3+}$ and *trans*-$[Ru^{III}L(H_2O)_2]^{3+}$ respectively. The rate constants k_{e1} and k_{e2} for the reduction of *trans*-$[Ru^{IV}L(OH)(H_2O)]^{3+}$ and *trans*-$[Ru^{III}L(H_2O)_2]^{3+}$ have been obtained and can be correlated with the Marcus cross-relation. The estimated self-exchange rate constants of the *trans*-$[RuL(OH)(H_2O)]^{3+/2+}$ and *trans*-$[RuL(H_2O)_2]^{3+/2+}$ couples are 3.1×10^{-4} and 3.9×10^{3} dm^3 mol^{-1} s^{-1} respectively. The complex *trans*-$[Ru^{III}L(OH)(H_2O)][ClO_4]_2$ has been characterised by X-ray crystallography: space group $P\bar{1}$, $a = 11.108(2)$, $b = 11.683(1)$, $c = 12.349(1)$ Å, $\alpha = 89.38(1)$, $\beta = 64.81(1)$, $\gamma = 71.44(1)°$ and $Z = 2$.

Oxoruthenium complexes are receiving attention because of their remarkable abilities in the stoichiometric and catalytic oxidation of organic substrates.[1] There are ample examples in the literature illustrating that monooxoruthenium-(IV) and -(V), *cis*- and *trans*-dioxoruthenium-(VI) and and -(V) having different redox potentials can readily be prepared.[1] Oxidation of substrates by these Ru=O complexes proceeds through various pathways, such as oxygen-atom transfer [2–4] and hydrogen [5] and hydride abstraction.[6]

In an attempt to elucidate the various factors governing the reactivities of Ru=O complexes in different oxidation states, we have begun a programme aiming at understanding the four-electron oxidation of *trans*-diaquaruthenium(II) to *trans*-dioxoruthenium(VI). Our previous work has established that *trans*-dioxoruthenium(VI) undergoes rapid one-electron reduction to give *trans*-dioxoruthenium(V) which then rapidly disproportionates in aqueous solutions.[7] The fast self-exchange rate constants of the redox couples *trans*-$[Ru^{VI}(tmc)O_2]^{2+}$–*trans*-$[Ru^{V}(tmc)O_2]^{+}$ and *trans*-$[Ru^{V}(tmc)O(OH)]^{2+}$–*trans*-$[Ru^{IV}(tmc)O(OH)]^{+}$ (tmc = 1,4,8,11-tetramethyl-1,4,8,11-tetraazacyclotetradecane) indicate small kinetic barriers for the redox interconversion, thus accounting for the reversibility of the two-electron redox couple *trans*-$[Ru^{VI}(tmc)O_2]^{2+}$–*trans*-$[Ru^{IV}(tmc)O(H_2O)]^{2+}$ in aqueous solution in cyclic voltammetric scans.[8]

It is well known that the redox couple Ru^{IV}=O/Ru^{III}–OH is usually irreversible at high concentration of H^+ and its reversibility can be strongly influenced by the nature and pretreatment of the electrode surface.[9] As noted,[9] the rate of oxidation of $[Ru^{III}(terpy)(bipy)(OH)]^{2+}$ (terpy = 2,2′:6′,2″-terpyridine, bipy = 2,2′-bipyridine) to $[Ru^{IV}(terpy)(bipy)O]^{2+}$ is slow at the electrode surface, being facilitated by the phenolic groups on the surface of a glassy carbon electrode. Our recent isolation of *trans*-$[Ru^{IV}L(O)(H_2O)][ClO_4]_2$ and *trans*-$[Ru^{III}L(OH)(H_2O)][ClO_4]_2$ [4a] (L = 6,7,8,9,10,11,17,18-octahydro-6,10-dimethyl-5*H*-dibenzo[*e*,*n*][1,4,8,12]dioxadiazacyclopentadecine) has prompted us to examine the mechanism of the two-electron reduction of Ru^{IV}=O to Ru^{II}–OH_2. The results of a kinetic study together with the X-ray structure of *trans*-$[Ru^{III}L(OH)(H_2O)][ClO_4]_2$ are reported here.

Experimental

Instrumentation.—The UV/VIS spectra were recorded on a Shimadzu UV-240 spectrophotometer. Cyclic voltammetry was performed on a Princeton Applied Research (PAR) model 273 potentiostat. Kinetic measurements were made with a Hi-Tech SF-51 stopped-flow module with a SU-40 spectrophotometric unit. The data collection process was controlled by an Apple IIe microcomputer *via* an ADS-1 interface unit, also from Hi-Tech.

Materials.—Water for kinetic studies was distilled twice from $KMnO_4$. Trifluoroacetic acid and trifluoromethanesulfonic acid were purified by distillation under a nitrogen atmosphere. Sodium trifluoroacetate (Aldrich) was recrystallized from ethanol and dried in a vacuum at 60 °C. The D_2O (99.9% D, Aldrich) and CF_3CO_2D (99% D, Aldrich) were used as received.

The compounds *trans*-$[Ru^{IV}L(O)(H_2O)][ClO_4]_2$,[4a] *trans*-$[Ru^{III}L(OH)(H_2O)][ClO_4]_2$,[4a] *cis*-$[Ru^{II}(NH_3)_4(isn)_2][ClO_4]_2$ (isn = isonicotinamide) [10] and $[Ru^{II}(NH_3)_4(bipy)][ClO_4]_2$ [11] were prepared according to literature procedures.

X-Ray Crystal Structure of trans-$[Ru^{III}L(OH)(H_2O)][ClO_4]_2 \cdot 2H_2O$.—X-Ray diffraction data were collected on an Enraf-Nonius CAD-4 diffractometer with graphite-monochromated Mo-Kα radiation ($\lambda = 0.710\,73$ Å) at 23 ± 1 °C. The unit-cell dimensions were obtained from a least-squares fit of 25 reflections in the range $20 < 2\theta < 34°$. The data were corrected for Lorentz polarization and absorption effects. The empirical absorption correction was based on (ψ) scans of six reflections with $80 < \chi < 90°$. Three check reflections, monitored every 2 h, showed no significant variation in intensity. Crystal and structure determination data are summarized in Table 1. Atomic scattering factors were taken from ref. 12. Calculations were carried out on a MicroVax II computer using the Enraf-Nonius SDP programs.

The position of the ruthenium atom was obtained from a Patterson synthesis, and the rest of the non-hydrogen atoms were revealed from a subsequent Fourier map. After several cycles of full-matrix least-squares refinement the hydrogen atoms were revealed in a Fourier difference map, however in the structure-factor calculation only those of the hydroxy group,

† *Supplementary data available:* see Instructions for Authors, *J. Chem. Soc., Dalton Trans.*, 1992, Issue 1, pp. xx–xxv.

Non-SI unit employed: cal = 4.184 J.

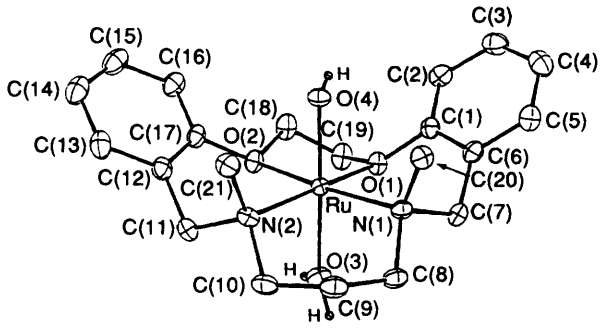

Fig. 1 An ORTEP plot of *trans*-$[Ru^{III}L(OH)(H_2O)]^{2+}$ cation

Table 1 Crystal and structure determination data for $[RuL(O)(H_2O)][ClO_4]_2 \cdot 2H_2O$

M	711.49
Crystal system	Triclinic
Space group	$P\bar{1}$ (no. 2)
a/Å	11.108(2)
b/Å	11.683(1)
c/Å	12.349(1)
α/°	89.38(1)
β/°	64.81(1)
γ/°	71.44(1)
U/Å^3	1360.2
Z	2
$F(000)$	730
D_c/g cm^{-3}	1.737
Crystal colour/shape	Yellow prism
Crystal dimensions/mm	0.19 × 0.19 × 0.10
μ/cm^{-1}	8.32
Transmission factors	0.924–0.999
Collection range	$\pm h, \pm k, \pm l$; $2\theta_{max} = 50°$
Scan mode and speed/° min^{-1}	ω–2θ, 0.8–5.5
Scan width/°	0.75 + 0.34tanθ
Background time	0.5 × scan time
No. of data collected	10 094
No. of unique data	4774
No. of data used in refinement, m	4089 [$I > 1.5\sigma(I)$]
R_{int}	0.016
No. of parameters refined, p	361
$R(F_o)$*	0.028
$R'(F_o)$*	0.037
S*	1.278
Maximum shift/error	0.06
Residual extrema in final difference map/e Å^{-3}	−0.54, +0.88

* $R = \Sigma||F_o| - |F_c||/\Sigma|F_o|$, $R' = [w(|F_o| - |F_c|)^2/\Sigma w|F_o|^2]^{\frac{1}{2}}$, with $w = 4F_o^2/[\sigma^2(F_o^2) + (0.04F_o^2)^2]$, $S = [\Sigma w(|F_c| - |F_c|)^2/(m - p)]^{\frac{1}{2}}$.

the methyl groups and the water molecules were taken while all the others were generated geometrically (C–H 0.95 Å). All non-hydrogen atoms were refined anisotropically and the hydrogen atoms with assigned isotropic thermal parameters (1.2 B_{eq} of the attached atom) were not refined.

Final agreement factors are shown in Table 1. Atomic coordinates of non-hydrogen atoms are given in Table 2, selected bond lengths and angles in Table 3.

Additional material available from the Cambridge Crystallographic Data Centre comprises H-atom coordinates, thermal parameters and remaining bond lengths and angles.

Reduction of trans-$[Ru^{IV}L(O)(H_2O)]^{2+}$ *by cis*-$[Ru^{II}(NH_3)_4(isn)_2]^{2+}$.—The kinetics was followed by monitoring the disappearance of the metal-to-ligand charge-transfer (m.l.c.t.) band of *cis*-$[Ru^{II}(NH_3)_4(isn)_2]^{2+}$ at 478 nm under the conditions that the concentration of *trans*-$[Ru^{IV}L(O)(H_2O)]^{2+}$ was in 50-fold excess of the ruthenium(II) reductant ($[Ru^{IV}] = 5 \times 10^{-4}$–$5 \times 10^{-3}$, $[Ru^{II}] = 1 \times 10^{-5}$–$1 \times 10^{-4}$ mol dm^{-3}). Pseudo-first-order rate constants k_{obs} were obtained by non-linear least-squares fit of absorbance A_t to time t according to the equation $(A_t - A_\infty) = (A_0 - A_\infty)\exp(-k_{obs}t)$. Each kinetic run was repeated at least 10 times and the mean value of k_{obs} was obtained. Second-order rate constants k_2 were obtained from linear least-squares fit of k_{obs} to $[Ru^{IV}]$.

Reduction of trans-$[Ru^{III}L(OH)(H_2O)]^{2+}$ *by* $[Ru^{II}(NH_3)_4(bipy)]^{2+}$.—The reaction conditions and kinetic data treatment were the same as described above. The reaction was followed by monitoring the disappearance of the m.l.c.t. band of $[Ru^{II}(NH_3)_4(bipy)]^{2+}$ at 523 nm under the conditions that the concentration of *trans*-$[Ru^{III}L(OH)(H_2O)]^{2+}$ was in 50-fold excess of the ruthenium(II) reductant ($[Ru^{III}] = 5 \times 10^{-4}$–$5 \times 10^{-3}$, $[Ru^{II}] = 1 \times 10^{-5}$–$1 \times 10^{-4}$ mol dm^{-3}).

Kinetic Isotopic Effect.—Several kinetic runs of the reduction of *trans*-$[Ru^{IV}L(O)(H_2O)]^{2+}$ by *cis*-$[Ru^{II}(NH_3)_4(isn)_2]^{2+}$ and of *trans*-$[Ru^{III}L(OH)(H_2O)]^{2+}$ by $[Ru^{II}(NH_3)_4(bipy)]^{2+}$ were carried out in CF_3CO_2D and D_2O ($[D^+] = 0.1$–0.5, $I = 0.5$ mol dm^{-3}).

Products and Stoichiometry.—The stoichiometries of the reactions were determined by measuring the UV/VIS spectrum of the ruthenium products after the reaction and by spectrophotometric redox titrations of *trans*-$[Ru^{IV}L(O)(H_2O)]^{2+}$ with *cis*-$[Ru^{II}(NH_3)_4(isn)_2]^{2+}$ and *trans*-$[Ru^{III}L(OH)(H_2O)]^{2+}$ with *cis*-$[Ru^{II}(NH_3)_4(bipy)]^{2+}$.

Results

Fig. 1 depicts an ORTEP plot of the *trans*-$[Ru^{III}L(OH)(H_2O)]^{2+}$ cation with atomic numbering scheme. Comparison of this with the structure of *trans*-$[Ru^{IV}L(O)(H_2O)]^{2+}$ reported earlier[4a] shows that the conformation and dimensions of these two cations and the Ru–N(L) and Ru–O(L) distances are very similar with only difference in the Ru^{III}–OH [1.905(2) Å] and Ru^{IV}=O [1.739(2) Å] bonds.[4a] Such a large difference is undoubtedly due to the difference in the extent of $p_\pi(O)$–d_π interaction, which is more pronounced in Ru^{IV}=O than in Ru^{III}–OH. The Ru–OH_2 distance of 2.102(2) Å in *trans*-$[Ru^{III}L(OH)(H_2O)]^{2+}$ is slightly shorter than that in *trans*-$[Ru^{IV}L(O)(H_2O)]^{2+}$ [2.199(3) Å],[4a] reflecting the greater *trans* effect of O^{2-} over OH^-. The average of the Ru–OH and Ru–OH_2 distances is 2.003 Å which is comparable to that of 2.007 Å reported by Meyer and co-workers[13] for the related *trans*-$[Ru^{III}(bipy)_2(OH)(H_2O)]^{2+}$.

The pH dependence of E° for the oxo–aqua–Ru–L system has been reported previously.[4a] In this work we have extended the studies at pH 0.3–3.0 ($I = 0.5$ mol dm^{-3}). Cyclic voltammetric scans under this condition revealed that the E° of the *trans*-$[RuL(OH)(H_2O)]^{3+/2+}$ couple is 0.66 ± 0.01 V *vs.* saturated calomel electrode (SCE) which appears to be insensitive to $[H^+]$ from 0.5 to 1.0 mol dm^{-3}. The E° for the *trans*-$[RuL(H_2O)_2]^{3+/2+}$ couple is similarly estimated to be 0.33 ± 0.01 V *vs.* SCE.

In the presence of an excess of *trans*-$[Ru^{IV}L(O)(H_2O)]^{2+}$ and in an aqueous acidic medium, *cis*-$[Ru^{II}(NH_3)_4(isn)_2]^{2+}$ was quantitatively oxidized to Ru^{III}. The decay of the ruthenium(II) reductant, monitored at 478 nm, was first order. The experimental results are fit very well by the equation $(A_t - A_\infty) = (A_0 - A_\infty)\exp(-k_{obs}t)$ and second-order rate constants k_2 were obtained from a linear least-squares fit of k_{obs} *vs.* $[Ru^{IV}]_T$ {$[Ru^{IV}]_T$ = total concentration of ruthenium(IV) species in the solution}. The rate law of the reaction is as in equation (1) where $k_{obs} = k_2[Ru^{IV}]_T$.

$$-d[Ru^{IV}]/dt = k_2[Ru^{IV}]_T[Ru^{II}] \quad (1)$$

Spectrophotometric titration indicated a stoichiometry of 1:1 [equation (2)].

Table 2 Fractional coordinates of non-hydrogen atoms and their estimated standard deviations (e.s.d.s) for $[RuL(OH)(H_2O)][ClO_4]_2 \cdot 2H_2O$

Atom	x	y	z	Atom	x	y	z
Ru	0.047 74(2)	0.187 29(2)	0.323 51(2)	C(14)	−0.177 8(3)	−0.107 0(3)	0.192 3(3)
O(1)	−0.091 0(2)	0.355 2(2)	0.433 2(2)	C(15)	−0.292 7(3)	−0.017 9(3)	0.278 1(3)
O(2)	−0.130 9(2)	0.211 2(2)	0.287 2(2)	C(16)	−0.281 7(3)	0.090 4(3)	0.312 6(3)
O(3)	0.113 5(2)	0.294 5(2)	0.184 5(2)	C(17)	−0.151 4(3)	0.105 0(3)	0.258 0(2)
O(4)	−0.040 3(2)	0.106 5(2)	0.453 0(2)	C(18)	−0.255 3(3)	0.301 9(3)	0.384 0(3)
N(1)	0.204 0(2)	0.186 8(2)	0.378 0(2)	C(19)	−0.212 3(3)	0.403 6(3)	0.406 8(3)
N(2)	0.175 6(2)	0.026 1(2)	0.199 0(2)	C(20)	0.220 6(3)	0.102 3(3)	0.466 5(2)
C(1)	−0.103 3(3)	0.372 9(2)	0.550 5(2)	C(21)	0.183 0(3)	−0.090 9(3)	0.251 5(2)
C(2)	−0.229 7(3)	0.404 2(3)	0.653 4(3)	Cl(1)	0.428 15(7)	0.308 85(7)	0.662 85(7)
C(3)	−0.228 2(3)	0.418 1(3)	0.764 0(3)	Cl(2)	−0.382 21(8)	0.341 74(8)	0.115 64(7)
C(4)	−0.101 8(3)	0.400 0(3)	0.769 9(3)	O(11)	0.459 6(2)	0.415 1(2)	0.626 5(3)
C(5)	0.023 7(3)	0.366 7(3)	0.664 7(3)	O(12)	0.306 3(3)	0.338 9(3)	0.778 2(3)
C(6)	0.025 8(3)	0.352 5(2)	0.553 3(2)	O(13)	0.395 9(3)	0.261 1(3)	0.577 7(3)
C(7)	0.161 7(2)	0.315 8(2)	0.437 5(2)	O(14)	0.547 7(3)	0.222 2(3)	0.666 1(3)
C(8)	0.346 3(3)	0.159 6(3)	0.272 0(2)	O(21)	−0.406 7(4)	0.462 9(3)	0.082 5(3)
C(9)	0.402 0(3)	0.037 0(3)	0.196 1(3)	O(22)	−0.238 9(3)	0.295 3(3)	0.095 3(3)
C(10)	0.324 6(3)	0.023 2(3)	0.124 6(3)	O(23)	−0.473 9(3)	0.349 4(3)	0.239 8(2)
C(11)	0.111 5(3)	0.028 8(3)	0.112 1(2)	O(24)	−0.404 4(3)	0.268 7(4)	0.043 5(3)
C(12)	−0.032 2(3)	0.015 3(3)	0.170 3(2)	O(5)	0.355 9(3)	0.289 7(3)	0.002 6(2)
C(13)	−0.047 2(3)	−0.091 4(3)	0.138 6(3)	O(6)	0.061 8(3)	0.578 8(3)	0.906 6(3)

Table 3 Selected bond lengths (Å) and angles (°) with e.s.d.s in parentheses

Ru–O(1)	2.102(2)	Ru–O(4)	1.904(2)
Ru–O(2)	2.148(2)	Ru–N(1)	2.110(3)
Ru–O(3)	2.126(3)	Ru–N(2)	2.105(2)
O(1)–Ru–O(2)	80.22(8)	O(2)–Ru–N(2)	93.90(9)
O(1)–Ru–O(3)	85.16(7)	O(3)–Ru–O(4)	171.12(7)
O(1)–Ru–O(4)	88.82(7)	O(3)–Ru–N(1)	93.25(9)
O(1)–Ru–N(1)	91.47(8)	O(3)–Ru–N(2)	90.71(8)
O(1)–Ru–N(2)	172.97(9)	O(4)–Ru–N(1)	93.4(1)
O(2)–Ru–O(3)	86.94(9)	O(4)–Ru–N(2)	94.61(8)
O(2)–Ru–O(4)	85.60(8)	N(1)–Ru–N(2)	94.44(9)
O(2)–Ru–N(1)	171.65(7)		

Table 4 Representative second-order rate constants for the reduction of *trans*-$[Ru^{IV}L(O)(H_2O)]^{2+}$ by *cis*-$[Ru^{II}(NH_3)_4(isn)_2]^{2+}$ at 298 K and $I = 0.50$ mol dm^{-3}

$[H^+]$/mol dm^{-3}	10^2k_2/dm^3 mol^{-1} s^{-1}
0.05	3.50 ± 0.20
0.10	3.97 ± 0.24
0.15	4.90 ± 0.27
0.20	5.25 ± 0.32
0.30	5.53 ± 0.34
0.40	5.76 ± 0.39

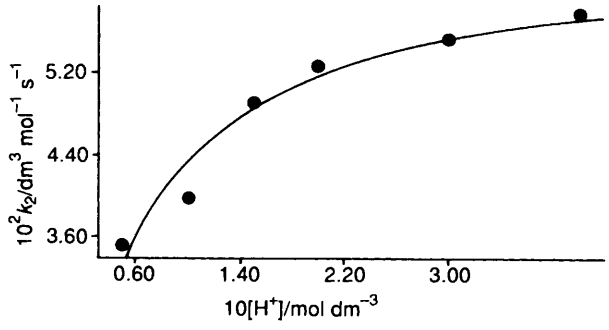

Fig. 2 Plot of k_2 *vs.* $[H^+]$ for the reduction of *trans*-$[Ru^{IV}L(O)(H_2O)]^{2+}$ at 298 K ($I = 0.5$ mol dm^{-3})

trans-$[Ru^{IV}L(O)(H_2O)]^{2+}$ + $[Ru^{II}(NH_3)_4(isn)_2]^{2+}$ + H^+ ⟶ *trans*-$[Ru^{III}L(OH)(H_2O)]^{2+}$ + $[Ru^{III}(NH_3)_4(isn)_2]^{3+}$ (2)

The effect of $[H^+]$ on k_2 has been investigated and the results are listed in Table 4. A plot of k_2 against $[H^+]$ ($[H^+] = 0.05$–0.5, $I = 0.5$ mol dm^{-3}) at 298 K is shown in Fig. 2. The kinetic data are consistent with Scheme 1, where protonation of *trans*-$[Ru^{IV}L(O)(H_2O)]^{2+}$ occurs prior to electron transfer.

trans-$[Ru^{IV}L(O)(H_2O)]^{2+}$ + H^+ $\overset{K_{p_1}}{\rightleftharpoons}$ *trans*-$[Ru^{IV}L(OH)(H_2O)]^{3+}$ (3)

trans-$[Ru^{IV}L(OH)(H_2O)]^{3+}$ + $[Ru^{II}(NH_3)_4(isn)_2]^{2+}$ $\xrightarrow{k_{e1}}$ *trans*-$[Ru^{III}L(OH)(H_2O)]^{2+}$ + $[Ru^{III}(NH_3)_4(isn)_2]^{3+}$ (4)

Scheme 1

In general, the rate of protonation [equation (3)] is diffusion-controlled. With this pre-equilibrium assumption, the rate law can be formulated as in equation (5). However, a pathway in

$$K_{p_1} = \frac{[Ru^{IV}L(OH)(H_2O)]^{3+}}{[H^+][Ru^{IV}L(O)(H_2O)]^{2+}}$$

$$-\frac{d[Ru^{II}]}{dt} = \frac{K_{p_1}k_{e1}[Ru^{II}][Ru^{IV}]_T[H^+]}{1 + K_{p_1}[H^+]}$$

$$k_{obs} = \frac{K_{p_1}k_{e1}[Ru^{IV}]_T[H^+]}{1 + K_{p_1}[H^+]}$$

$$k_2 = \frac{K_{p_1}k_{e1}[H^+]}{1 + K_{p_1}[H^+]} \quad (5)$$

which protonation occurs after electron transfer cannot be completely ruled out (Scheme 2).

trans-$[Ru^{IV}(O)(H_2O)]^{2+}$ + $[Ru^{II}(NH_3)_4(isn)_2]^{2+}$ ⟶ *trans*-$[Ru^{III}L(O)(H_2O)]^{+}$ + $[Ru^{III}(NH_3)_4(isn)_2]^{3+}$ (6)

trans-$[Ru^{III}L(O)(H_2O)]^{+}$ + H^+ ⟶ *trans*-$[Ru^{III}L(OH)(H_2O)]^{2+}$ (7)

Scheme 2

Electrochemically, we have not been able to locate the $Ru^{IV}{=}O/Ru^{III}{=}O$ couple. The $E^{\ominus}$ of the reaction $[Ru^{IV}L(O)(H_2O)]^{2+}$ + e^- ⟶ $[Ru^{III}L(O)(H_2O)]^{+}$ should occur at a very negative potential because $Ru^{III}{=}O$ is such an unfavour-

Table 5 Temperature dependence of k_{e1} for reduction of *trans*-$[Ru^{IV}L(O)(H_2O)]^{2+}$ by *cis*-$[Ru^{II}(NH_3)_4(isn)_2]^{2+}$ (I = 0.5 mol dm^{-3})

T/K	k_{e1}/dm^3 mol^{-1} s^{-1}
289.5 ± 0.1	399 ± 15
298.0 ± 0.1	641 ± 26
298.0 ± 0.1	534 ± 21 *
307.7 ± 0.1	881 ± 19
316.8 ± 0.1	1284 ± 74

* Reaction was carried out in CF_3CO_2D–D_2O.

Table 6 Representative second-order rate constants for the reduction of *trans*-$[Ru^{III}L(OH)(H_2O)]^{2+}$ by $[Ru^{II}(NH_3)_4(bipy)]^{2+}$ at different $[H^+]$ (I = 0.2 mol dm^{-3}) at 298 K

$[H^+]$/mol dm^{-3}	$10^{-4}k_2$/dm^3 mol^{-1} s^{-1}
0.01	0.61 ± 0.02
0.02	1.27 ± 0.05
0.03	1.85 ± 0.11
0.04	2.35 ± 0.16
0.06	3.21 ± 0.20
0.08	3.93 ± 0.26
0.10	4.69 ± 0.32
0.12	5.52 ± 0.34
0.15	6.15 ± 0.44
0.18	6.36 ± 0.42
0.20	6.50 ± 0.45

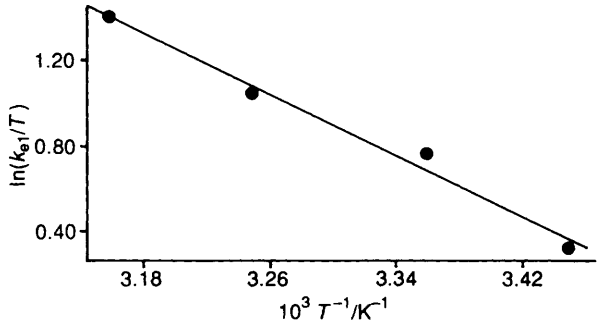

Fig. 3 Eyring plot for the reduction of *trans*-$[Ru^{IV}L(O)(H_2O)]^{2+}$ by *cis*-$[Ru^{II}(NH_3)_4(isn)_2]^{2+}$

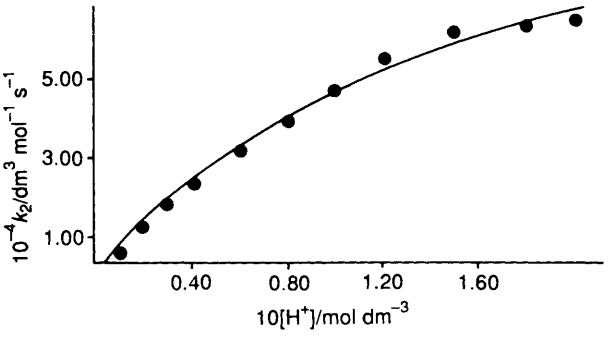

Fig. 4 Plot of k_2 *vs.* $[H^+]$ for the reduction of *trans*-$[Ru^{III}L(OH)(H_2O)]^{2+}$ at 298 K (I = 0.2 mol dm^{-3})

able geometry for Ru^{III}. Our electrochemical study[14] showed that *trans*-$[Ru^{IV}L(O)(MeCN)]^{2+}$ undergoes an irreversible reduction at potential of −1.45 V *vs.* Ag–$AgNO_3$ in acetonitrile. Thus, although the reduction of *trans*-$[Ru^{IV}L(O)(H_2O)]^{2+}$ to *trans*-$[Ru^{III}L(OH)(H_2O)]^{2+}$ by $[Ru^{II}(NH_3)_4(isn)_2]^{2+}$ is an overall downhill reaction at pH ≤7, reaction (6) in Scheme 2 should be thermodynamically uphill by at least 0.26 V. Of course, such a reaction could be driven to the product side by subsequent protonation of *trans*-$[Ru^{III}L(O)(H_2O)]^{+}$. In this

Table 7 Temperature dependence of k_{e2} for the reduction of *trans*-$[Ru^{III}L(OH)(H_2O)]^{2+}$ by $[Ru^{II}(NH_3)_4(bipy)]^{2+}$ (I = 0.2 mol dm^{-3})

T/K	10^{-4} k_{e2}/dm^3 mol^{-1} s^{-1}
287.0 ± 0.1	7.7 ± 0.4
298.0 ± 0.1	9.8 ± 0.5
298.0 ± 0.1	9.0 ± 0.5 *
307.0 ± 0.1	11.7 ± 0.6
318.0 ± 0.1	13.4 ± 0.7

* Reaction carried out in CF_3CO_2D–D_2O.

sense, the endergonic reaction is driven by a strongly exergonic subsequent reaction. If the reduction follows Scheme 2, $[Ru^{III}(NH_3)_4(isn)_2]^{3+}$, once generated, will also be reduced back to $[Ru^{II}(NH_3)_4(isn)_2]^{2+}$. Reaction (6) may not be a true equilibrium and the disappearance of $[Ru^{II}(NH_3)_4(isn)_2]^{2+}$ will not follow a simple first-order decay. In this work, a clean first-order decay of $[Ru^{II}(NH_3)_4(isn)_2]^{2+}$ was observed. Under our experimental conditions ($[H^+]$ = 0.1–0.5 mol dm^{-3}) and given the fact that the pK_a value of *trans*-$[Ru^{IV}L(O)(H_2O)]^{2+}$ has been found to be 1.32 (see later), the major ruthenium species in the solution is *trans*-$[Ru^{IV}L(OH)(H_2O)]^{3+}$. By cyclic voltammetry, the E° of the reversible *trans*-$[Ru^{IV}L(OH)(H_2O)]^{3+}$–*trans*-$[Ru^{III}L(OH)(H_2O)]^{2+}$ couple has been estimated to be 0.66 ± 0.01 V *vs.* SCE. Thus reaction (4) is a downhill reaction with a ΔG° of −4.6 kcal mol^{-1}. Hence, it is unlikely that under our reaction conditions the reduction follows Scheme 2.

A non-linear least-squares fit of the kinetic data at I = 0.5 mol dm^{-3} and 298 K (Fig. 2) according to equation (5) leads to k_{e1} = 641 ± 26 dm^3 mol^{-1} s^{-1} and K_{p_1} = 20.9 ± 1.6 dm^3 mol^{-1} (pK_a = 1.32 ± 0.20).

The k_{e1} values for the reduction of *trans*-$[Ru^{IV}L(O)(H_2O)]^{2+}$ at different temperatures are listed in Table 5. The $\Delta H^\ddagger$ and $\Delta S^\ddagger$ values found from a plot of $\ln(k_e/T)$ against $1/T$ (Fig. 3) are 7.1 ± 0.5 kcal mol^{-1} and −22 ± 2 cal K^{-1} mol^{-1} respectively.

A kinetic isotopic effect of 1.2 was found for the reduction of *trans*-$[Ru^{IV}L(O)(H_2O)]^{2+}$ at I = 0.5 mol dm^{-3} and 298 K.

For the reduction of *trans*-$[Ru^{III}L(OH)(H_2O)]^{2+}$ by $[Ru^{II}(NH_3)_4(bipy)]^{2+}$, the decay of the ruthenium(II) reductant is also first order. The rate law is as in equation (8).

$$-d[Ru^{II}]/dt = k_2[Ru^{III}][Ru^{II}] \quad (8)$$

where $k_{obs} = k_2[Ru^{III}]$. Spectrophotometric titration at 0.1 mol dm^{-3} in CF_3CO_2H indicated a stoichiometry of 1:1, in accordance with equation (9).

$$trans\text{-}[Ru^{III}L(OH)(H_2O)]^{2+} + [Ru^{II}(NH_3)_4(bipy)]^{2+} + H^+ \longrightarrow trans\text{-}[Ru^{II}L(H_2O)_2]^{2+} + [Ru^{III}(NH_3)_4(bipy)]^{3+} \quad (9)$$

The k_2 values obtained at different $[H^+]$ (I = 0.2 mol dm^{-3}, 298 K) are listed in Table 6 and a plot of k_2 *vs.* $[H^+]$ is shown in Fig. 4. The results are consistent with Scheme 3 where k_2 is

$$trans\text{-}[Ru^{III}L(OH)(H_2O)]^{2+} + H^+ \overset{K_{p_2}}{\rightleftharpoons} trans\text{-}[Ru^{III}L(H_2O)_2]^{3+} \quad (10)$$

$$trans\text{-}[Ru^{III}L(H_2O)_2]^{3+} + [Ru^{II}(NH_3)_4(bipy)]^{2+} \xrightarrow{k_{e2}} trans\text{-}[Ru^{II}L(H_2O)_2]^{2+} + [Ru^{III}(NH_3)_4(bipy)]^{3+} \quad (11)$$

Scheme 3

given by expression (12). A non-linear least-squares fit of the kinetic data (Fig. 4) according to equation (12) gave the

Table 8 Summary of kinetic rate data for the calculation of self-exchange rate constants for the Ru^{IV}–Ru^{III} and Ru^{III}–Ru^{II} couples

Couple	E/V *vs.* NHE	K_{12}	k_{12} / dm^3 mol^{-1} s^{-1}	k_{22}	k_{11}
$[RuL(OH)(H_2O)]^{3+/2+}$	0.90	2.4×10^3	6.4×10^{-2}	7.7×10^5	3.1×10^{-4}
$[Ru(NH_3)_4(isn)_2]^{3+/2+}$	0.70				
$[RuL(H_2O)_2]^{3+/2+}$	0.57	3.22	9.8×10^4	7.7×10^5	3.9×10^3
$[Ru(NH_3)_4(bipy)]^{3+/2+}$	0.54				

Table 9 Comparison of ΔG_{in}^{*} and the self-exchange rate constant for the electron-exchange reaction of Ru^{III}–Ru^{II} and Ru^{IV}–Ru^{III} couples at 25 °C

Exchange reaction	$2r_A$[a]/Å	$2r_B$[a]/Å	ΔG_{in}[b]/ kcal mol^{-1}	k_{self}/dm^3 mol^{-1}
$[Ru(NH_3)_6]^{3+/2+}$	6.6		6.82	4.7×10^3
$[Ru(NH_3)_5(py)]^{3+/2+}$	7.6		5.92	1.1×10^3
$[Ru(NH_3)_4(bipy)]^{3+/2+}$	8.8		5.11	7.7×10^5
$[Ru(NH_3)_2(bipy)_2]^{3+/2+}$	11.2		4.02	8.4×10^7
$[RuL(H_2O)_2]^{3+/2+}$	7.76	7.94	5.74	3.9×10^3
$[RuL(OH)(H_2O)]^{3+/2+}$	7.74	7.76	5.81	3.1×10^{-4}

[a] Calculated from equation (16). [b] Calculated from equation (15).

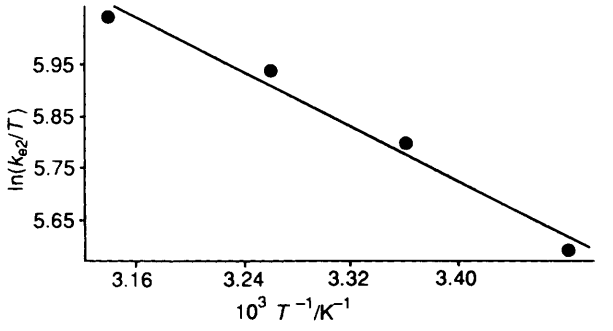

Fig. 5 Eyring plot for the reduction of *trans*-$[Ru^{III}L(OH)(H_2O)]^{2+}$ by $[Ru^{II}(NH_3)_4(bipy)]^{2+}$

$$k_2 = \frac{k_{e2}K_{p_2}[H^+]}{1 + K_{p_2}[H^+]} \quad (12)$$

respective k_{e2} and K_{p_2} values (9.8 ± 0.5) × 10^4 dm^3 mol^{-1} s^{-1} and 9.6 ± 0.8 dm^3 mol^{-1}. The k_{e2} values at different temperatures are summarized in Table 7. From the Eyring plot of $\ln(k_{e2}/T)$ against $1/T$ (Fig. 5), the $\Delta H^{\ddagger}$ and $\Delta S^{\ddagger}$ for the reduction reaction are 2.8 ± 0.2 kcal mol^{-1} and −26 ± 3 cal K^{-1} mol^{-1} respectively. A kinetic isotopic effect of 1.1 was obtained.

From the results of the reduction of *trans*-$[Ru^{IV}L(O)(H_2O)]^{2+}$ and *trans*-$[Ru^{III}L(OH)(H_2O)]^{2+}$ by the one-electron reductants, the mechanism for the reduction of Ru^{IV} to Ru^{II} of the Ru–L–oxo–aqua system can be summarized as Scheme 1 followed by Scheme 3.

Discussion

In this work the one-electron reduction of H_2O–Ru^{IV}=O to H_2O–Ru^{III}–OH and of H_2O–Ru^{III}–OH to H_2O–Ru^{II}–OH_2 at high $[H^+]$ involves prior protonation with the intermediates being *trans*-$[Ru^{IV}L(OH)(H_2O)]^{3+}$ and *trans*-$[Ru^{II}L(H_2O)_2]^{3+}$. Since the protonated forms are involved in the reactions, the question arises as to what type of redox reactions are involved since a proton can serve as a bridge for the two reactants through intermolecular hydrogen bonding in the transition state. However the small kinetic isotopic effects of 1.2 [equation (4)] and 1.1 [equation (11)] suggest that H-atom transfer is unimportant in the rate-determining step. Furthermore, the activation parameters for these two reactions are similar to those found in other outer-sphere one-electron-transfer reactions.[11,15] The larger $\Delta H^{\ddagger}$ for the reduction of *trans*-$[Ru^{IV}L(O)(H_2O)]^{2+}$ is in agreement with the slower self-exchange rate constant of the Ru^{IV}=OH/Ru^{III}–OH couple as described later.

Assuming a simple adiabatic outer-sphere electron-transfer mechanism, values for the self-exchange rate constants of the Ru^{IV}–Ru^{III} and Ru^{III}–Ru^{II} couples can be estimated by the well known Marcus cross-relation (13) in which k_{12} is the rate

$$k_{12} = (k_{11}k_{22}K_{12}f_{12})^{\frac{1}{2}} \quad (13)$$

$$\ln f_{12} = \frac{\ln K_{12}}{4\ln(k_{11}k_{22}/Z^2)} \quad (14)$$

constant for the cross reaction, k_{11} and k_{22} are the exchange rate constants of the reactants, K_{12} is the equilibrium constant for the cross reaction and $Z = 1 \times 10^{11}$ dm^3 mol^{-1} s^{-1}.[16,17] The E° of the *trans*-$[Ru^{IV}L(OH)(H_2O_2)]^{3+}$–*trans*-$[Ru^{III}L(OH)(H_2O)]^{2+}$ and *trans*-$[Ru^{III}L(H_2O)_2]^{3+}$–*trans*-$[Ru^{II}L(H_2O)_2]^{2+}$ couples are 0.66 and 0.33 V *vs.* SCE respectively at an ionic strength of 0.5 mol dm^{-3}. The E° values for the ruthenium(II) reductants have also been redetermined at the pH range at which the kinetic experiments were performed. Table 8 summarizes the kinetic data and the E° values for the calculation of self-exchange rate constants. The self-exchange rate constant of the *trans*-$[Ru(L)(H_2O)_2]^{3+/2+}$ couple {refer to the reaction *trans*-$[Ru^{III}L(H_2O)_2]^{3+}$ + e^- ⟶ *trans*-$[Ru^{II}L(H_2O)_2]^{2+}$} is 3.9 × 10^3 dm^3 mol^{-1} s^{-1}. This value is comparable to that of 4.3 × 10^3 dm^3 mol^{-1} s^{-1} for $[Ru(NH_3)_6]^{3+/2+}$,[11] but considerably smaller than the values[11] for $[Ru(NH_3)_5(py)]^{3+/2+}$ (py = pyridine) (1.1 × 10^5 dm^3 mol^{-1} s^{-1}), $[Ru(NH_3)_4(bipy)]^{3+/2+}$ (7.7 × 10^5 dm^3 mol^{-1} s^{-1}) and $[Ru(NH_3)_2(bipy)_2]^{3+/2+}$ (8.4 × 10^7 dm^3 mol^{-1} s^{-1}). A direct comparison between the *trans*-$[RuL(H_2O)_2]^{3+/2+}$ and $[Ru(OH_2)_6]^{3+/2+}$ couples (60 dm^3 mol^{-1} s^{-1})[18] revealed that the latter has a much smaller self-exchange rate constant. This may be due to the smaller outer-sphere reorganization energy for the former couple. The outer-sphere reorganization energy for the reaction *trans*-$[Ru^{III}L(H_2O)_2]^{3+}$ + e^- ⟶ *trans*-$[Ru^{II}L(H_2O)_2]^{2+}$ [equation (15)] has been estimated using

$$\Delta G^{*}_{out} = \tfrac{1}{4}e^2[(1/\eta^2) - (1/D_s)][(1/2r_A) + (1/2r_B) - (1/r_{AB})] \quad (15)$$

crystal data for *trans*-$[Ru^{III}L(OH)(H_2O)][ClO_4]_2$ and *trans*-$[Ru^{II}L(NH_3)_2][ClO_4]_2$.[19] Here η and D_s are the refractive index and static dielectric constant of the solvent respectively, r_{AB} is the separation of the metal centres in the activated complex (assumed equal to $r_A + r_B$) and r_A and r_B are the radii of the two reactants. The Ru^{II}–OH_2 bond distance was assumed to be 2.1 Å.[20] Since equation (15) is for spherical reactants, we have calculated the radii equivalent to spheres of equal volume using the relation (16) where d_i (i = 1,2,3) are the diameters along the three axes of the reactant. The outer-sphere

$$r = \tfrac{1}{2}(d_1d_2d_3)^{\frac{1}{3}} \quad (16)$$

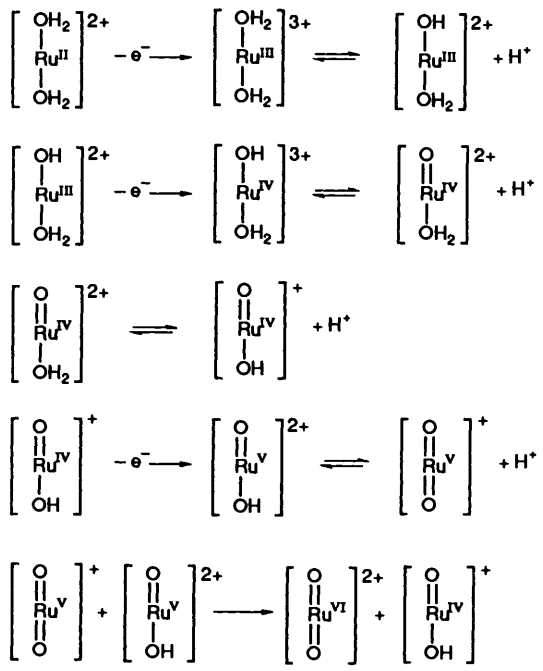

Scheme 4

reorganization energies for some Ru^{III}–Ru^{II} couples are listed in Table 9. A value of 5.74 kcal mol^{-1} is estimated for the *trans*-$[RuL(H_2O)_2]^{3+/2+}$ couple, which is smaller than those of 6.82 and 5.92 kcal mol^{-1} for $[Ru(NH_3)_6]^{3+/2+}$ and $[Ru(NH_3)_5(py)]^{3+/2+}$ respectively.[11] Usually a smaller reorganization energy means a faster self-exchange rate, but the *trans*-$[RuL(H_2O)]^{3+/2+}$ couple has a smaller self-exchange rate constant than those for $[Ru(NH_3)_6]^{3+/2+}$ and $[Ru(NH_3)_5(py)]^{3+/2+}$. This could be due to a larger inner-sphere reorganization energy. Previous work also suggested that the redox couple $[Ru(H_2O)_6]^{3+/2+}$ has a larger inner-sphere reorganization energy than that of $[Ru(NH_3)_6]^{3+/2+}$.[18] This has been attributed to a smaller change in metal–ligand bond distances: $[Ru(NH_3)_6]^{3+/2+}$, Δ(Ru–NH_3), 0.04 Å;[21] $[Ru(H_2O)_6]^{3+/2+}$, Δ(Ru–OH_2) ≈ 0.1 Å.[20]

To our knowledge, there are no prior self-exchange rate data for Ru^{IV}–Ru^{III} couples. In this work, the self-exchange rate constants for the *trans*-$[RuL(OH)(H_2O)]^{3+/2+}$ couple is 3.1×10^{-4} dm^3 mol^{-1} s^{-1}. Such a slow self-exchange rate is consistent with the higher $\Delta H^{\ddagger}$ obtained for the reduction of *trans*-$[Ru^{IV}L(OH)(H_2O)]^{3+/2+}$ than that for the reduction of *trans*-$[RuL(H_2O)_2]^{3+/2+}$. From crystal data for *trans*-$[Ru^{IV}L(O)(H_2O)][ClO_4]_2$[4a] and *trans*-$[Ru^{III}L(OH)(H_2O)][ClO_4]_2$, an outer-sphere reorganization energy of 5.81 kcal mol^{-1} is estimated from equations (15) and (16) for the reduction of *trans*-$[Ru^{IV}L(OH)(H_2O)]^{3+}$ to *trans*-$[Ru^{III}L(OH)(H_2O)]^{2+}$, which is comparable to the value of 5.74 kcal mol^{-1} for the reduction of *trans*-$[Ru^{III}L(H_2O)_2]^{3+}$ to *trans*-$[Ru^{II}L(H_2O)_2]^{2+}$. The X-ray structures of *trans*-$[Ru^{IV}L(O)(H_2O)]^{2+}$ and *trans*-$[Ru^{III}L(OH)(H_2O)]^{2+}$ show a large difference in bond length between the Ru^{IV}=O (1.739 Å)[4a] and Ru^{III}–OH (1.904 Å) group. Although quantitative values for the $\Delta G_{in}^{\ddagger}$ cannot be obtained as the Ru^{IV}=OH bond length has not been determined by X-ray crystallography, the extremely slow self-exchange rate for the *trans*-$[RuL(OH)(H_2O)]^{3+/2+}$ couple suggests a large Frank–Condon barrier associated with the reduction of Ru^{IV}=OH to Ru^{III}–OH and hence Ru^{IV}=OH should be formulated as a double bond and may have a comparable bond distance to Ru^{IV}=O.

Conclusion

The oxidation of *trans*-diaquaruthenium(II) to *trans*-dioxoruthenium(VI) in an aqueous acidic medium proceeds through five steps (Scheme 4). Kinetic studies revealed that the most difficult part lies in the oxidation of Ru^{III} to Ru^{IV}, which has the largest reorganization energy. This accounts for the fact that in cyclic voltammetric scans the Ru^{IV}–Ru^{III} couple is usually irreversible at high $[H^+]$. The design of new oxoruthenium(IV) complexes with higher Ru^{IV}–Ru^{III} self-exchange rate constants is the subject of our future research in this area.

Acknowledgements

We thank the University and Polytechnic Granting Committee, the Croucher Foundation and University of Hong Kong for support.

References

1 W. P. Griffith, *Transition Met. Chem.*, 1990, **15**, 251.
2 J. C. Dobson, W. K. Seok and T. J. Meyer, *Inorg. Chem.*, 1986, **25**, 1513; B. A. Moyer, B. K. Sipe and T. J. Meyer, *Inorg. Chem.*, 1981, **20**, 1475; L. Roecker, J. C. Dobson, W. J. Vining and T. J. Meyer, *Inorg. Chem.*, 1987, **26**, 779.
3 S. Perrier, T. C. Lau and J. K. Kochi, *Inorg. Chem.*, 1990, **29**, 4190; J. T. Groves and R. Quinn, *J. Am. Chem. Soc.*, 1985, **107**, 5790; C. L. Bailey and R. S. Drago, *J. Chem. Soc., Chem. Commun.*, 1987, 179.
4 (*a*) C. M. Che, W. T. Tang, W. T. Wong and T. F. Lai, *J. Am. Chem. Soc.*, 1989, **111**, 9048; (*b*) C. Ho, W. H. Leung and C. M. Che, *J. Chem. Soc., Dalton Trans.*, 1991, 2933.
5 L. Roecker and T. J. Meyer, *J. Am. Chem. Soc.*, 1987, **109**, 746; M. S. Thompson and T. J. Meyer, *J. Am. Chem. Soc.*, 1982, **104**, 5070; C. M. Che, C. Ho and T. C. Lau, *J. Chem. Soc., Dalton Trans.*, 1991, 1259; C. M. Che, W. T. Tang, K. Y. Wong and C. K. Li, *J. Chem. Soc., Dalton Trans.*, 1991, 3277.
6 R. A. Binstead, B. A. Moyer, G. J. Samuels and T. J. Meyer, *J. Am. Chem. Soc.*, 1981, **103**, 2897; R. A. Binstead and T. J. Meyer, *J. Am. Chem. Soc.*, 1987, **109**, 3287; C. M. Che, W. H. Leung, C. K. Li and C. K. Poon, *J. Chem. Soc., Dalton Trans.*, 1991, 379.
7 C. M. Che, K. Lau, T. C. Lau and C. K. Poon, *J. Am. Chem. Soc.*, 1990, **112**, 5176.
8 C. M. Che, K. Y. Wong and F. C. Anson, *J. Electroanal. Chem., Interfacial Electrochem.*, 1987, **226**, 211.
9 R. C. McHatton and F. C. Anson, *Inorg. Chem.*, 1984, **23**, 3935; G. E. Cabaniss, A. A. Diamantis, W. R. Murphy, jun., R. W. Linton and T. J. Meyer, *J. Am. Chem. Soc.*, 1985, **107**, 1845.
10 R. G. Gaunder and H. Taube, *Inorg. Chem.*, 1970, **9**, 2627.
11 G. M. Brown and N. Sutin, *J. Am. Chem. Soc.*, 1979, **101**, 883.
12 *International Tables for X-Ray Crystallography*, Kynoch Press, Birmingham, 1974, vol. 4, pp. 72, 149.
13 B. Durham, S. R. Wilson, D. J. Hodgson and T. J. Meyer, *J. Am. Chem. Soc.*, 1980, **102**, 600.
14 W. T. Tang, Ph.D. Thesis, University of Hong Kong, 1989.
15 G. M. Brown, H. J. Krentzien, M. Abe and H. Taube, *Inorg. Chem.*, 1979, **18**, 3374.
16 R. A. Marcus, *J. Chem. Phys.*, 1956, **24**, 4966; 1965, **43**, 679.
17 R. A. Marcus, *J. Phys. Chem.*, 1963, **67**, 853; 1968, **72**, 891.
18 W. Böttcher, G. M. Brown and N. Sutin, *Inorg. Chem.*, 1979, **6**, 1447.
19 W. F. Tong, unpublished work.
20 P. Bernhard, H.-B. Burgi, J. Hauser, H. Lehmann and A. Ludi, *Inorg. Chem.*, 1982, **21**, 3936.
21 H. C. Stynes and J. A. Ibers, *Inorg. Chem.*, 1971, **10**, 2304.

Received 17*th September* 1991; *Paper* 1/04800G